ELECTRONIC SUPPLEMENTARY INFORMATION

Cascade Chiral Amine Synthesis Catalyzed by Site-Specifically Co-Immobilized Alcohol and Amine Dehydrogenases

Si Liu, Zhenfu Wang, Kun Chen, Linling Yu, Qinghong Shi, Xiaoyan Dong, Yan Sun*

Department of Biochemical Engineering, School of Chemical Engineering and Technology and Key Laboratory of Systems Bioengineering and Frontiers Science Center for Synthetic Biology (Ministry of Education), Tianjin University, Tianjin 300350, China

*E-mail: ysun@tju.edu.cn

Number of pages: 30

Number of Tables: 10

Number of Figures: 16

Number of Supplementary Experimental Procedures: 4

Table S1. List of protein sequences for fused- and non-fused enzymes.

ADH from *Aromatoleum aromaticum* (previously named as denitrifying bacterium strain EbN1)[1]
MTQRLKDKLAVITGGANGIGRAIAERFAVEGADIAIADLVPAPEAEAAIRNLG RRVLTVKCDVSQPGDVEAFGKQVISTFGRCDILVNNAGIYPLIPFDELTFEQW KKTFEINVDSGFLMAKAFVPGMKRNGWGRIINLTSTTYWLKIEAYTHYISTKA ANIGFTRALASDLGKDGITVNAIAPSLVRTATTEASALSAMFDVLPNMLQAIP RLQVPLDLTGAAAFLASDDASFITGQTLAVDGGMVRH
AmDH: Chimera of *Bacillus stearothermophilus* Leu-DH and *Bacillus badius* PheDH[2]
MSLVEKTSIIKDFTLFEKMSEHEQVVFCNDPATGLRAIIAIHDTTLGPALGGCR MQPYNSVEEALEDALRLSKGMTYSCAASDVDFGGGKAVIIGDPQKDKSPELF RAFGQFVDSLGGRFYTGTDMGTNMEDFIHAMKETNCIVGVPEAYGSSGNPSP ATAYGVYRGMKAAAKEAFGSDSLEGKVVAVQGVGNVAYHLCRHLHEEGA KLIVTDINKEAVARAVEEFGAKAVDPNDIYGVECDIFAPCALGGIINDQTIPQL KAKVIAGSALNQLKEPRHGDMIHEMGIVYAPDYVINAGGCINVADELYGYNR ERAMKKIEQIYDNIEKVFAIAKRDNIPTYVAADRMAEERIETMRKARSQFLQN GHHILSRRRAR
SiBP-(G₄S)₂-ADH
SGRARAQRQSSRGRGGGGSGGGGSMTQRLKDKLAVITGGANGIGRAIAERFA VEGADIAIADLVPAPEAEAAIRNLGRRVLTVKCDVSQPGDVEAFGKQVISTFG RCDILVNNAGIYPLIPFDELTFEQWKKTFEINVDSGFLMAKAFVPGMKRNGW GRIINLTSTTYWLKIEAYTHYISTKAANIGFTRALASDLGKDGITVNAIAPSLVR TATTEASALSAMFDVLPNMLQAIPRLQVPLDLTGAAAFLASDDASFITGQTLA VDGGMVRH
SiBP-(G₄S)₂-AmDH
SGRARAQRQSSRGRGGGGSGGGGSMSLVEKTSIIKDFTLFEKMSEHEQVVFC NDPATGLRAIIAIHDTTLGPALGGCRMQPYNSVEEALEDALRLSKGMTYSCA ASDVDFGGGKAVIIGDPQKDKSPELFRAFGQFVDSLGGRFYTGTDMGTNMED FIHAMKETNCIVGVPEAYGSSGNPSPATAYGVYRGMKAAAKEAFGSDSLEGK VVAVQGVGNVAYHLCRHLHEEGAKLIVTDINKEAVARAVEEFGAKAVDPND IYGVECDIFAPCALGGIINDQTIPQLKAKVIAGSALNQLKEPRHGDMIHEMGIV YAPDYVINAGGCINVADELYGYNRERAMKKIEQIYDNIEKVFAIAKRDNIPTY VAADRMAEERIETMRKARSQFLQNGHHILSRRRAR

Table S2. Preparation of six co-immobilized dual-enzyme systems (Co-IEs), one mixed free enzyme (M-FE), and one mixed single-immobilized enzyme (S-IE) and corresponding enzyme loadings.

	SiBP-ADH (µM)	SiBP-AmDH (µM)	SNPs (mg/mL)	SiBP-ADH loading (mg protein/g SNPs)	SiBP-AmDH loading (mg protein/g SNPs)
Co-IE-1	0.69	4.5	5	3.8 ± 0.04	30.1 ± 0.3
Co-IE-2	0.35	4.5	5	1.9 ± 0.03	37.8 ± 0.3
Co-IE-3	0.28	4.5	5	1.6 ± 0.02	38.3 ± 0.5
Co-IE-4	0.23	4.5	5	1.3 ± 0.02	39.9 ± 0.2
Co-IE-5	0.28	4.5	10	0.8 ± 0.01	20.0 ± 0.3
Co-IE-6	0.28	4.5	15	0.5 ± 0.01	13.3 ± 0.1
Co-IE-7	0.28	4.5	20	0.4 ± 0.02	10.0 ± 0.2
M-FE	0.28	4.5	0	-	-
S-IE	0.28	4.5	10	0.8 ± 0.02	20.0 ± 0.1

Table S3. GC retention time of substrates and products under the conditions [a] used in this work.

Entry	Compound	GC column	Retention time (min)
1	(*S*)-2-hexanol	DB-1701	9.17
2	2-hexanone	DB-1701	8.27
3	(*R*)-2-aminohexane	DB-1701	5.96
4	(*R*)-2- aminohexane	DEX-CB	6.88
5	(*S*)-2- aminohexane	DEX-CB	6.33

[a] The substances of entries 1 – 3 were detected by GC-MS with the following operational parameters: injector 250 °C; temperature program: 40 °C/hold 8 min; 100 °C/rate 20 °C min^{-1}/hold 1 min; 280 °C/rate 20 °C min^{-1}/hold 1 min. The substances of 4 and 5 entries were detected by GC-MS with the following operational parameters: injector 200 °C; temperature program: 60 °C/hold 8 min; 100 °C/rate 5 °C min^{-1}/hold 2 min; 180 °C/rate 10 °C min^{-1}/hold 1 min.

Table S4. Expression levels of wild-type and recombinant proteins.

Enzyme	Expression level (mg/L)
ADH	1786 ± 189
SiBP-ADH	1340 ± 103
AmDH	5547 ± 676
SiBP-AmDH	6670 ± 429

Table S5. Particle size and specific surface area of SNPs.

	Particle size (nm)	Specific surface area [a] (m^2/g)
SNPs	18.5 ± 1.6	147 ± 13

[a] The specific surface area of SNPs was calculated according to the following equation,

$$\text{Specific surface area} = \frac{6}{d\rho}$$

where d represents the diameter of SNPs (m), ρ is the density of SNPs (silica density 2.2 g/mL^3). Therefore, the specific surface area of SNPs was calculated at 147 m^2/g.

Table S6. Adsorption equilibrium parameters of recombinant proteins onto SNPs.

	K_d (mg/mL)	q_m (mg/g)
SiBP-ADH	$3.10 \times 10^{-5} \pm 0.5 \times 10^{-5}$	380 ± 15
SiBP-AmDH	$1.76 \times 10^{-2} \pm 0.01$	522 ± 19
GFP-SiBP [a]	$\sim 3.80 \times 10^{-5}$	~ 25.1

[a] Data from literature on silica particles (α-quartz) with a diameter of approximately 0.8 μm.[4]

Table S7. Effect of initial protein concentration on SiBP-AmDH loading onto SNPs.

Initial SiBP-AmDH concentration (mg/mL)	0.005	0.01	0.05	0.1	0.2	0.5	1
Protein loading (mg protein/g SNPs)	1.0 ± 0.1	2.0 ± 0.1	10.0 ± 0.7	19.2 ± 1.6	38.0 ± 0.4	83.8 ± 1.3	165.0 ± 2.1
Immobilization efficiency (%)	100.0 ± 0.1	100.0 ± 0.1	100.0 ±2.1	96.2 ± 4.9	94.9 ± 0.9	83.8 ±0.6	82.6 ±1.1

Table S8. Results of co-immobilization at different dual-enzyme molar ratios at a definite SiBP-AmDH enzyme concentration.

Ratio of dual-enzyme [a]	Final SiBP-ADH concentration (µM)	Total loaded protein (mg protein/g SNPs)	Immobilization efficiency (%)
1:7	0.69	38.4 ± 0.3	87.3 ± 2.7
1:13	0.35	39.7 ± 0.3	94.6 ± 2.8
1:16	0.28	39.9 ± 0.5	96.2 ± 4.8
1:20	0.23	41.2 ± 0.2	99.7 ± 0.2

[a] Dual-enzyme molar ratio was defined as SiBP-ADH:SiBP-AmDH and the concentration of SiBP-AmDH was maintained at 4.5 µM.

Table S9. Total turnover numbers (TTNs) [a] of NAD$^+$ with different dual-enzyme cascade catalytic systems during 48 h reaction.

(S)-2-Hexanol (mM)	10	20	30
M-FE	5	10	20
S-IE	6	12	21
Co-IE	9	17	23

[a] TTNs were calculated according to the following equation.

$$TTN = \frac{\mu mol\ produced\ end\text{-}product}{\mu mol\ of\ NAD^+\ in\ reaction}$$

Example from Table S8, second row, second column:

$$produced\ end\text{-}product\ [mmol] = \frac{48\%\ conv.}{100} * 10\ mM * 0.1\ mL = 0.48\ \mu mol$$

$$TTN = \frac{0.48\ \mu mol}{1 * 0.1\ \mu mol} \approx 5$$

Table S10. Calculation of *E*-factor for this work and literatures. [a]

Reference	5	6	7	This work
Carrier (mg)		17.5	N.D. [b]	10.0
ADH (mg)	40.0	0.17	2.0 [c]	0.008
AmDH (mg)		6.48	50.0 [d]	0.20
Other enzymes	No	No	15.0 [e]	No
Substrate (mg)	3.07	2.04	23.0 [f]	3.06
NAD(H) (mg)	0.66	0.66	0.007	0.66
NH$_4$Cl (mg)	107	107	26.7	107
Total amount of waste (mg)	150.7	133.9	116.7	120.9
Mass of product (mg)	2.45	1.86	2.12	2.28
E-factor	62	72	55	53

[a] Total volume of the catalytic system is 1 mL. [b] No data available. [c] The weight of cells carrying ADH. [d] The weight of AmDH-MNPs. [e] GDH-MNPs applies for NADH regeneration. [f] Substrates are 4-phenyl-2-butanol (3 mg, primary substrate) and glucose (20 mg, sacrificial substrate).
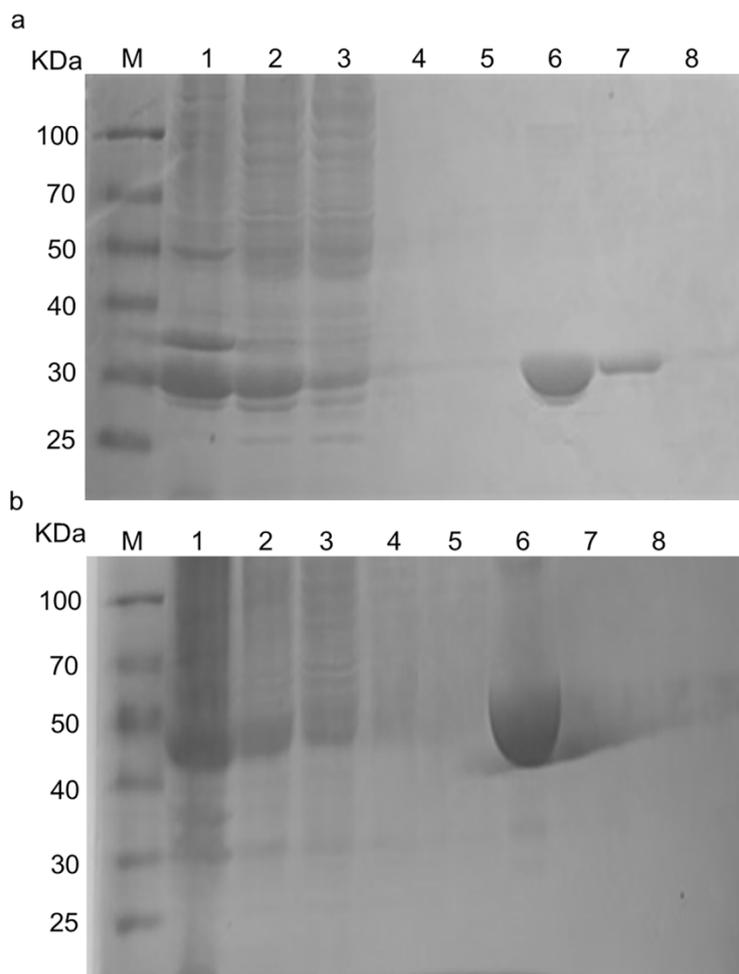
Fig. S1 Expression and purification of recombinant proteins analyzed by SDS-PAGE. (a) SiBP-ADH, (b) SiBP-AmDH. M, protein marker; Lane 1, bacterial crushing precipitation; Lane 2, bacterial crushing supernatant; Lane 3, sample loading penetration solution; Lanes 4 – 5, elution solution; Lane 6, elution solution; Lanes 7 – 8, column regeneration solution. The purity of the protein was analyzed by Image Lab[TM] Software version 5.2.1 (Bio-Rad, Hercules, CA, USA).[8]
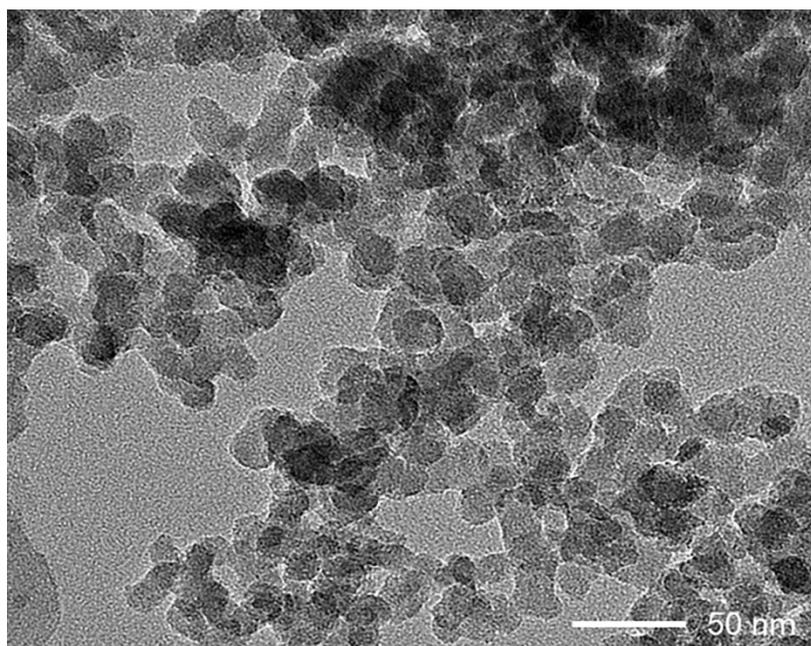
Fig. S2 A TEM image of SNPs.
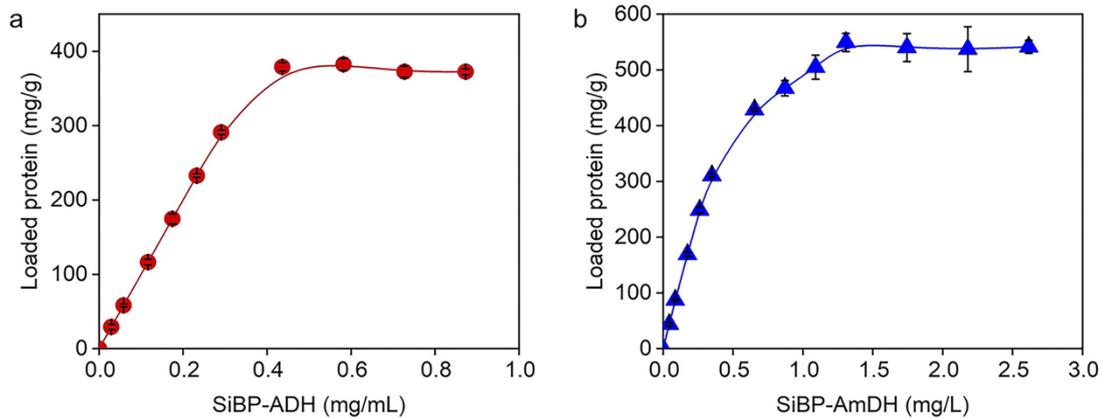
Fig. S3 Effect of added protein concentration on the immobilization of (a) SiBP-ADH and (b) SiBP-AmDH onto SNPs. All experiments were conducted in triplicate, and mean values with standard deviations are reported.
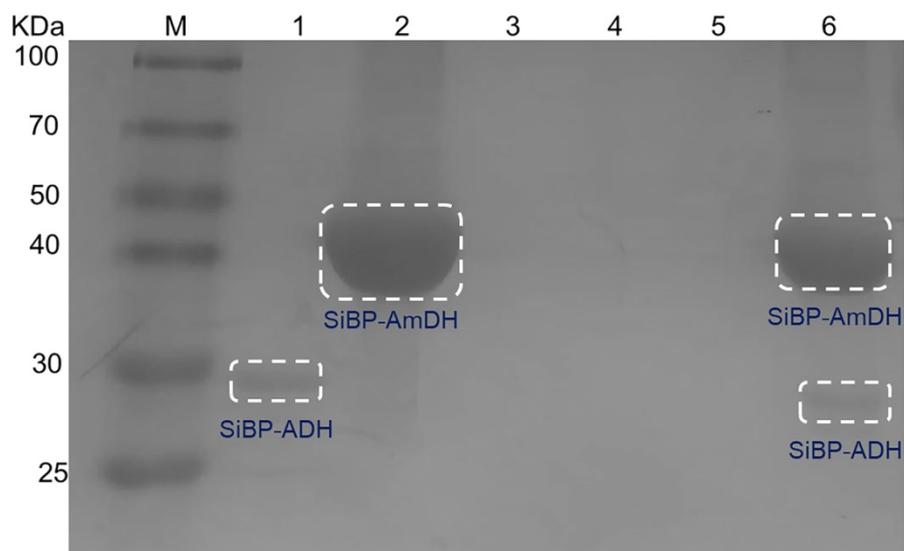
Fig. S4 SDS-PAGE analysis of the preparation of SiBP-ADH@SNPs and SiBP-AmDH@SNPs. M: Protein standard; Lane 1: purified SiBP-ADH before immobilization; Lane 2: purified SiBP-AmDH before immobilization; Lane 3: supernatant after immobilization; Lanes 4 and 5: wash solutions; Lane 6: co-immobilized dual-enzyme released from SNPs after the treatments by boiling in SDS buffer.
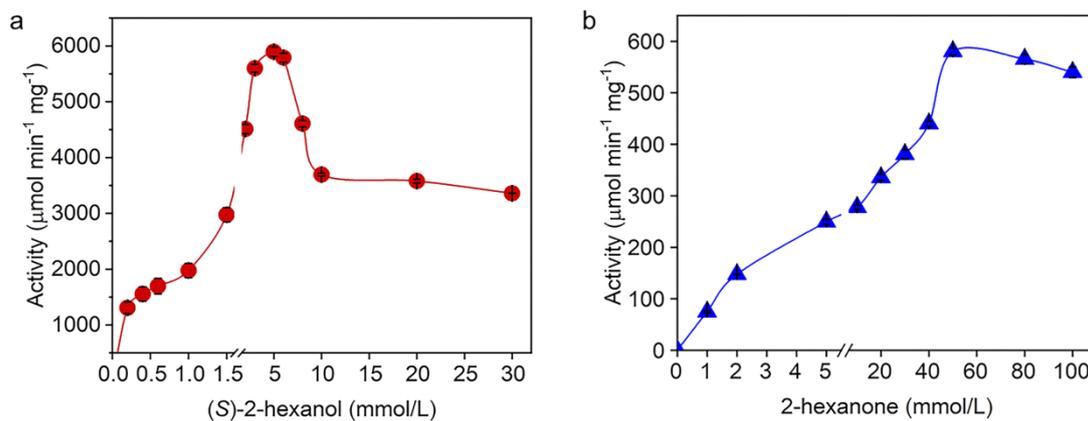
Fig. S5 Activities of (a) SiBP-ADH and (b) SiBP-AmDH as a function of substrate concentration. Enzymatic reactions were conducted with 0.02 mg/mL SiBP-ADH or 0.2 mg/mL SiBP-AmDH and 1 mM NAD(H). Error bars represent the standard deviation of triplicate experiments.
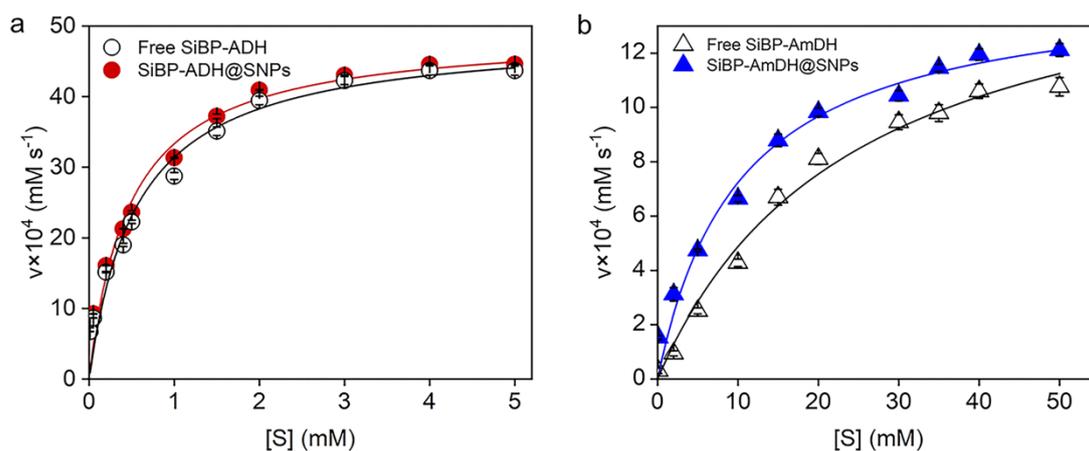
Fig. S6. Reaction rates of (a) SiBP-ADH and (b) SiBP-AmDH as a function of substrate concentration. Solid lines are calculated from the Michaelis-Menten equation with kinetic parameters listed in **Table 1**. The activities of free and immobilized SiBP-ADH/SiBP-AmDH were measured at (*S*)-2-hexanol concentration range from 0 - 5 mM (for SiBP-ADH) and 2-hexanone concentration range from 0 - 50 mM (for SiBP-AmDH). The results were the average of three independent experiments.
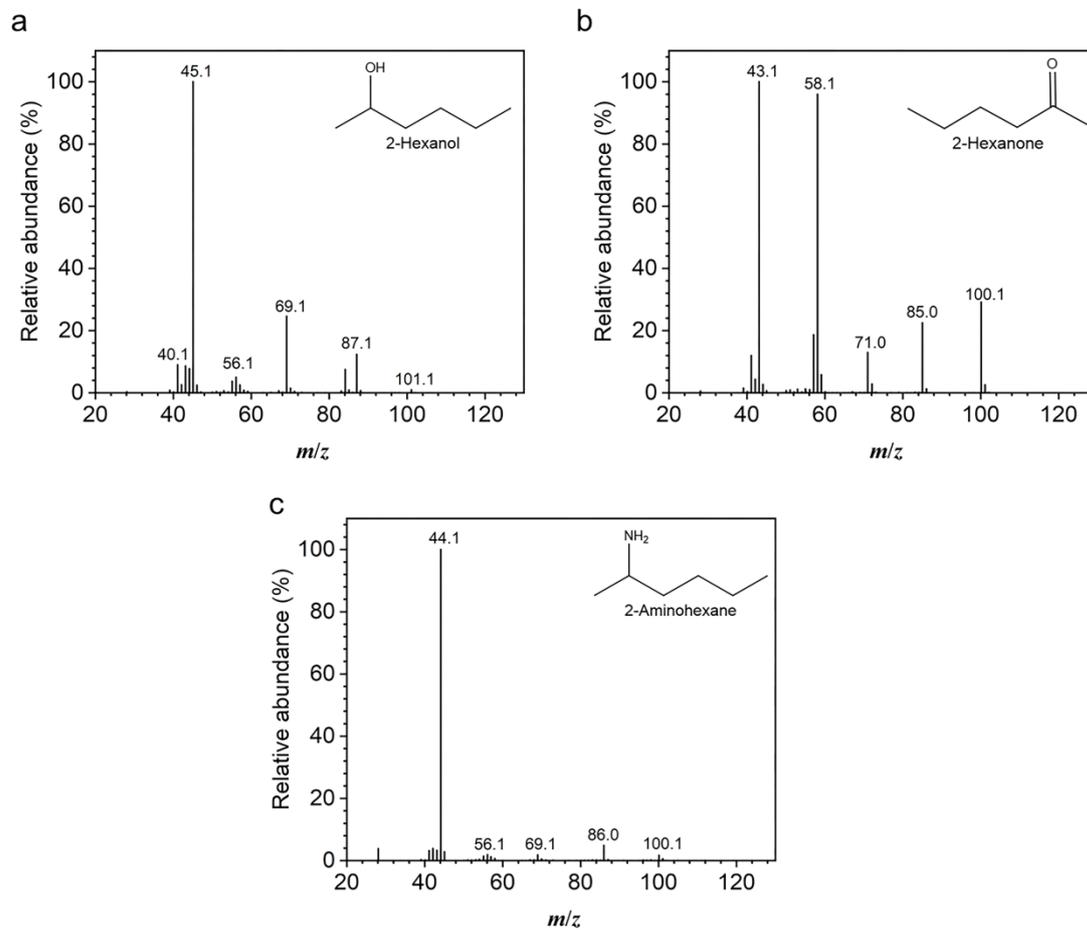
Fig. S7 GC-MS analysis of substrate, intermediate product, and final product extracted from the cascade amination reaction systems.
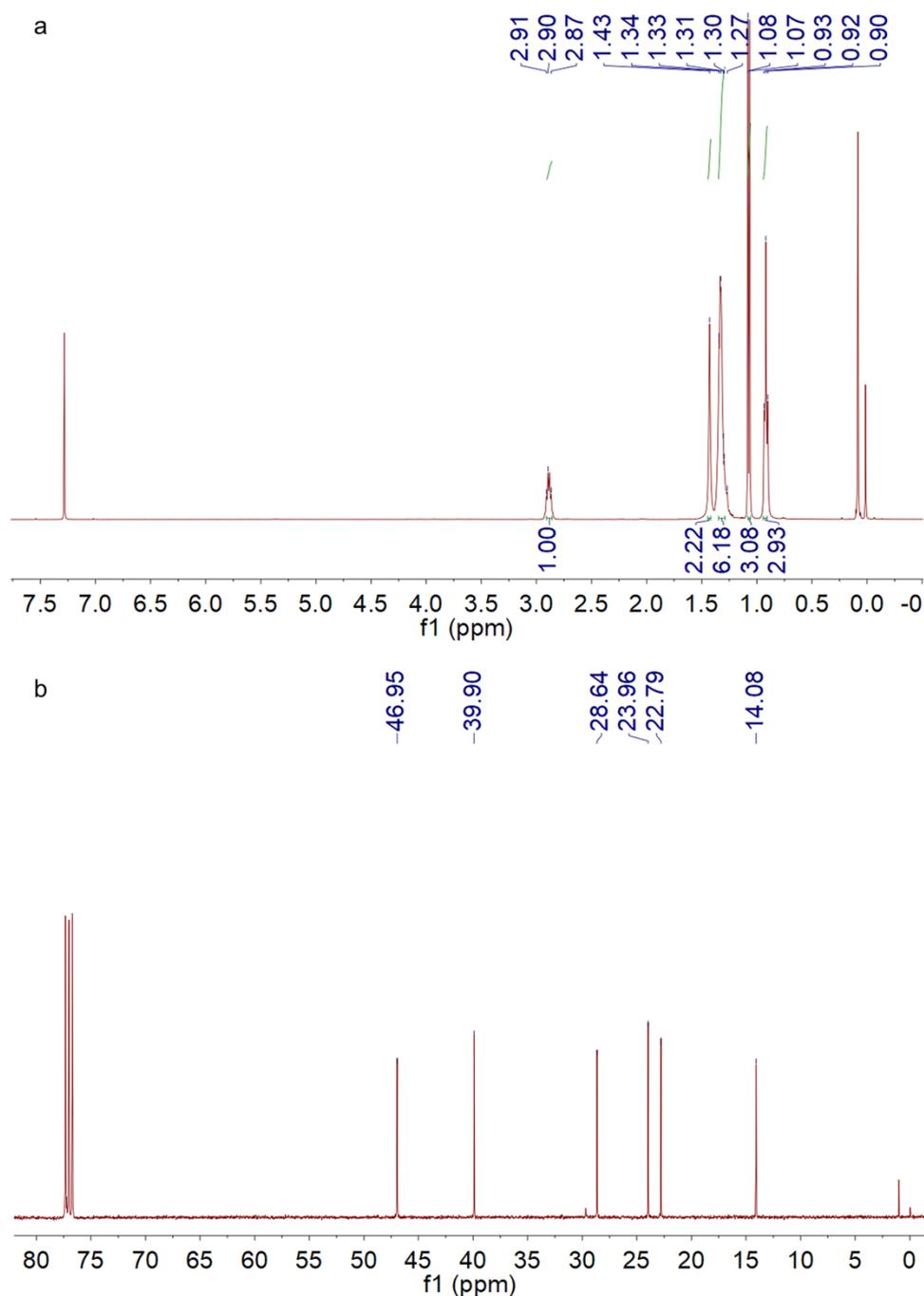
Fig. S8 Spectral data for hydrocarbons analysis of (*R*)-2-aminohexane by NMR. (a) ¹H NMR of (*R*)-2-aminohexane. (b) ¹³C NMR of (*R*)-2-aminohexane.

¹H NMR (500 MHz, CDCl₃): δ 2.90 (t, *J* = 10.0 Hz, 1H), 1.43 (s, 2H), 1.38 – 1.25 (m, 6H), 1.08 (d, *J* = 5.0 Hz, 3H), 0.92 (t, *J* = 7.5 Hz, 3H); ¹³C NMR (500 MHz, CDCl₃): δ 46.95, 39.90, 28.64, 23.96, 22.79, 14.08; in agreement with literature.[9]
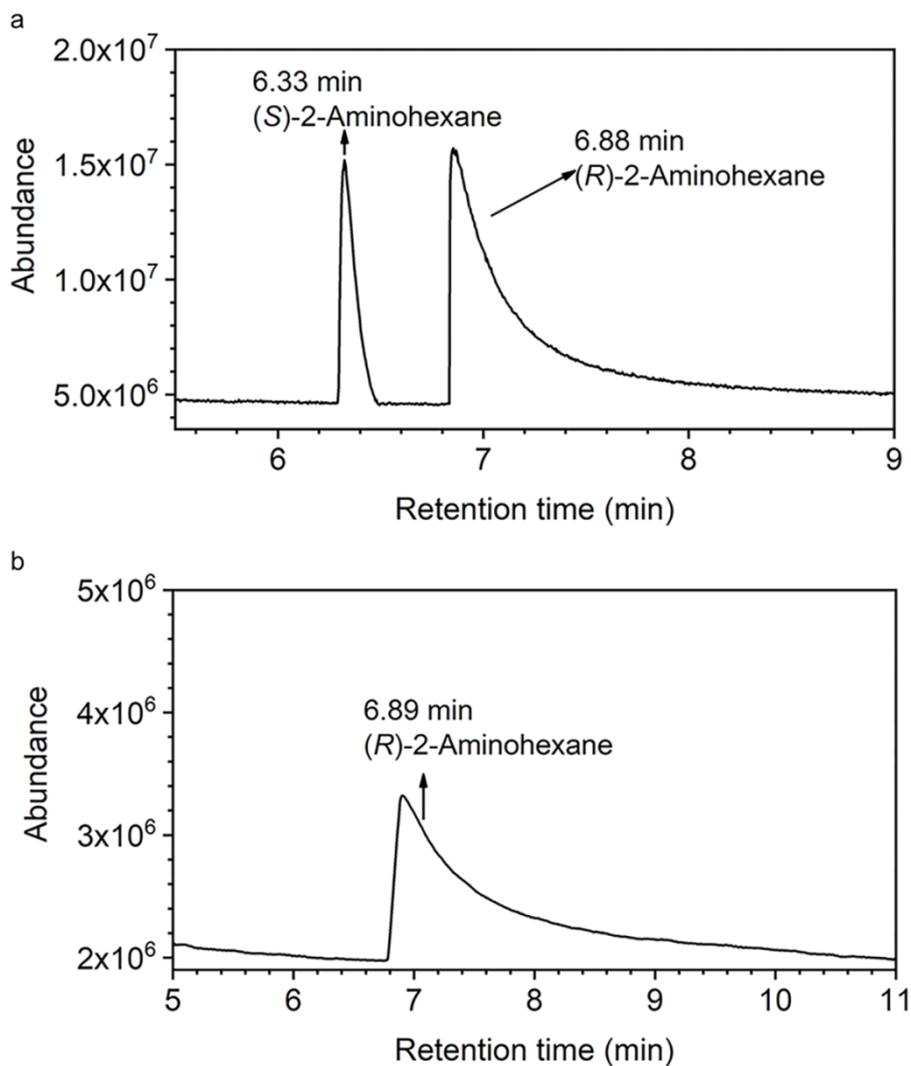
Fig. S9 Determination of the enantiomeric excess of the 2-aminohexane product by gas chromatography analysis. (a) Chromatogram of commercially available (*S*)-2-aminohexane and (*R*)-2-aminohexane. (b) Chromatogram of (*R*)-2-aminohexane produced by the Co-IE system. Note that the above substances were derivatized prior to GC-MS analysis. The derivative process see section S3.1.
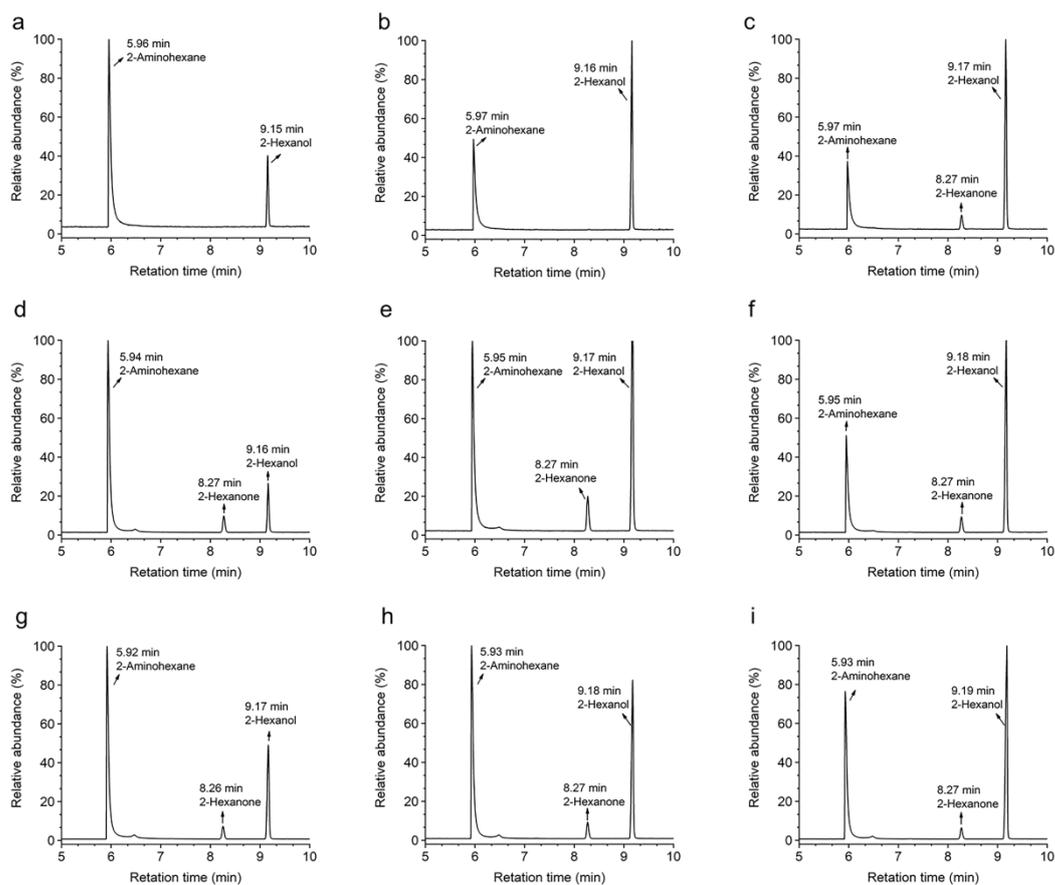
Fig. S10 Gas chromatography analysis of amination cascade reaction with (a, d, and g) Co-IE, (b, e, and h) S-IE, and (c, f, and i) M-FE systems at different substrate concentrations. The concentrations of (*S*)-2-hexanol were (a to c) 10 mM, (d to f) 20 mM, and (g to i) 30 mM. The chromatographic profiles reflect the amount of substrate and products in different catalytic systems after 48 h reaction.
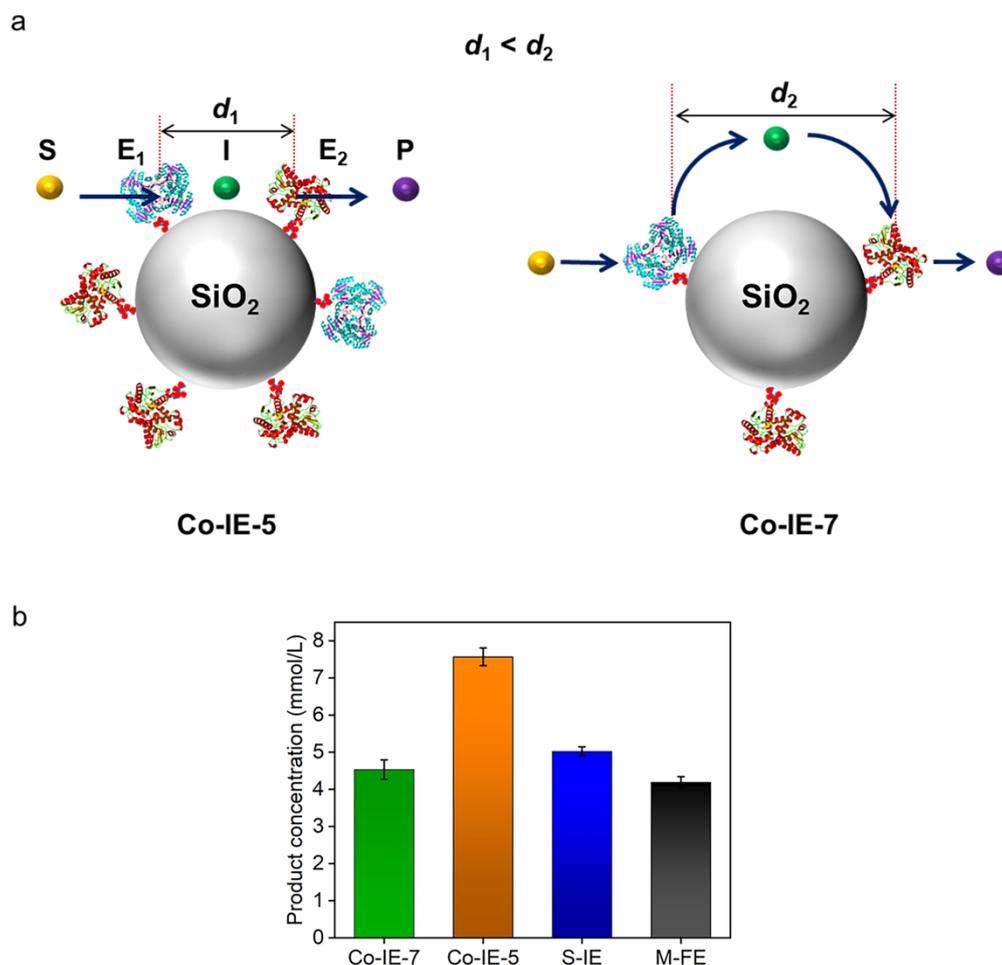
Fig. S11 Investigation of the proximity effect in the Co-IE system. (a) Illustration of cascade reaction processes with Co-IE-5 (left) and Co-IE-7 (right) systems at different enzyme densities. Co-IE-5 and Co-IE-7 were prepared as listed in Table S2. The enzyme density of Co-IE-5 was two-fold higher than that of Co-IE-7. E_1, E_2, S, I, P, d_1, and d_2 refers to enzyme 1 (SiBP-ADH), enzyme 2 (SiBP-AmDH), substrate [(S)-2-hexanol and NAD^+], intermediate (2-hexanone and NADH), product [(R)-2-aminohexane and NAD^+], distance 1, and distance 2, respectively. (b) Product yields of (R)-2-aminohexane with different ADH+AmDH cascade systems. Product concentrations were determined after reactions for 24 h. All cascade reactions were performed with 10 mM (S)-2-hexanol and 1 mM NAD^+. Error bars represent standard deviations of triplicate experiments.
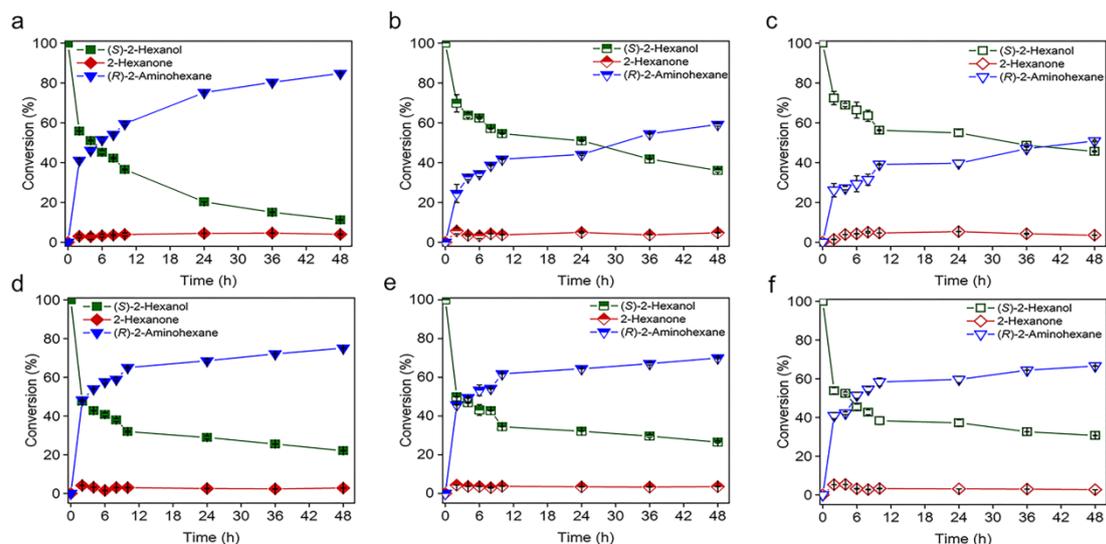
Fig. S12 Time course of amination reaction by different cascade catalytic systems at (a - c) 20 mM or (d - f) 30 mM (*S*)-2-hexanol. The catalytic systems were (a and d) Co-IE, (b and e) S-IE, and (c and f) M-FE. All cascade reactions were performed with 1 mM NAD^+ at 30 °C and 190 rpm. Conversion rates are shown as the percentage (%) of alcohol converted to ketone intermediate and final amine product. Error bars represent the standard deviation of three experiments.
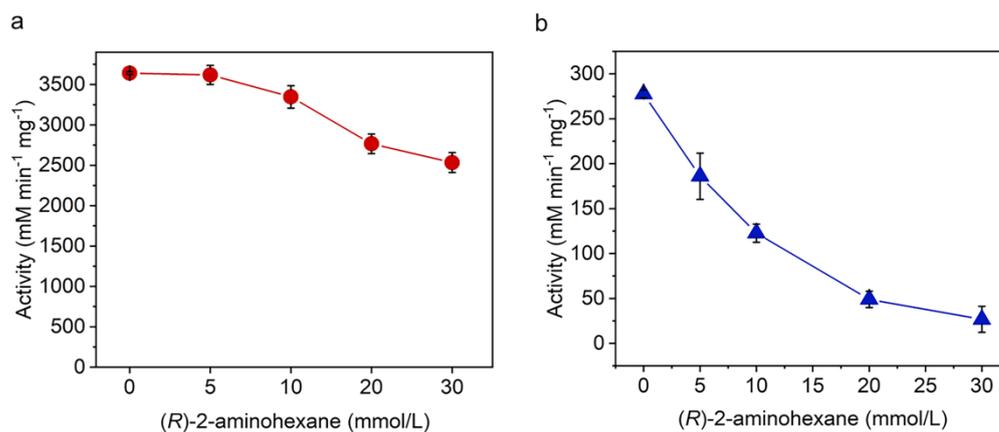
Fig. S13 Activities of (a) SiBP-ADH and (b) SiBP-AmDH as a function of product concentration. Enzymatic reactions were conducted with 0.02 mg/mL SiBP-ADH or 0.2 mg/mL SiBP-AmDH, 1 mM NAD(H), and 10 mM substrate. Error bars represent standard deviations of triplicate experiments.
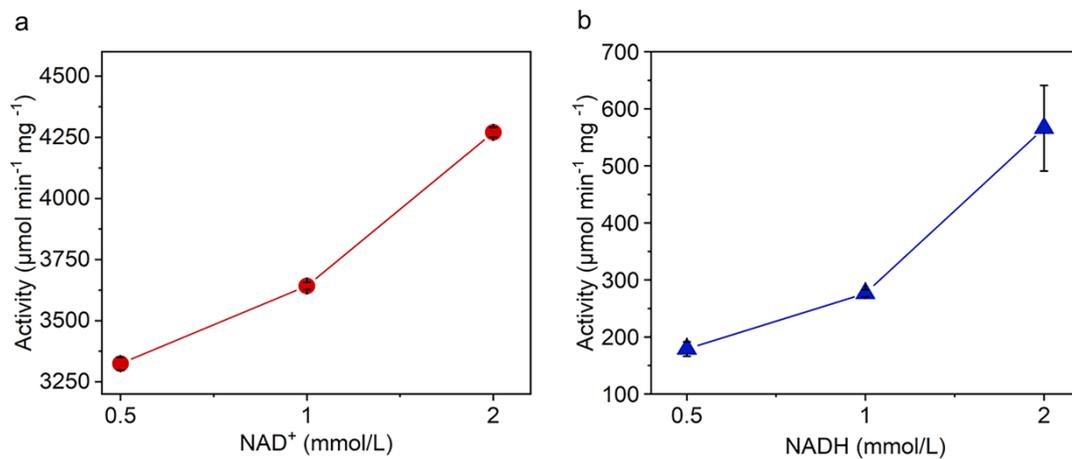
Fig. S14 Activities of (a) SiBP-ADH and (b) SiBP-AmDH as a function of NAD(H) concentration. Enzymatic reactions were conducted with 0.02 mg/mL SiBP-ADH or 0.2 mg/mL SiBP-AmDH and 10 mM substrate. Error bars represent standard deviations of triplicate experiments.
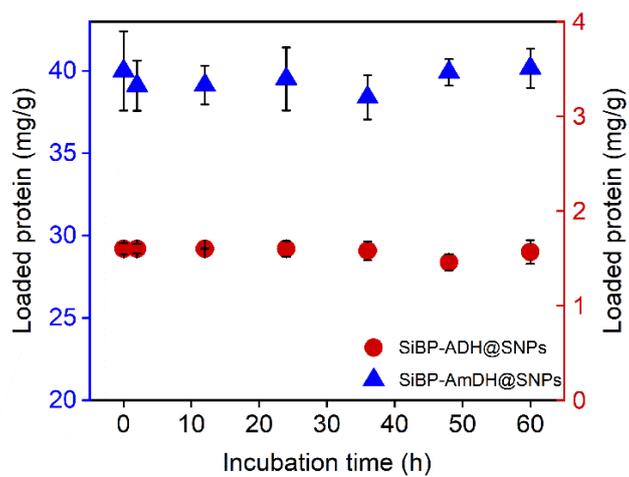
Fig. S15 Bound protein stability of SiBP-ADH@SNPs and SiBP-AmDH@SNPs on the particles at 30 ℃.
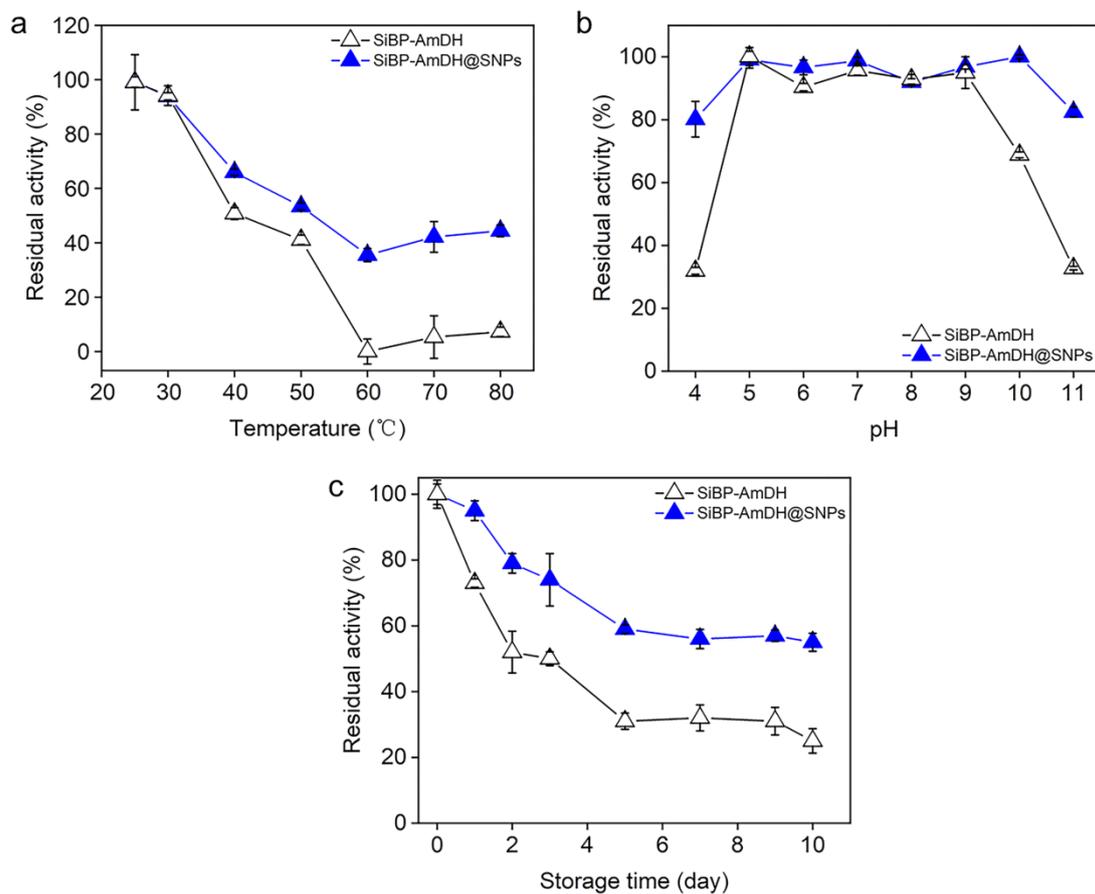
Fig. S16 Stability of free and immobilized SiBP-AmDH. (a) Thermal stability of SiBP-AmDH and SiBP-AmDH@SNPs. (b) The pH tolerance of SiBP-AmDH and SiBP-AmDH@SNPs. (c) Storage stability of SiBP-AmDH and SiBP-AmDH@SNPs at 4 °C. The activity was determined using 2-hexanone as substrate. All experiments were conducted in triplicate, and mean values with standard deviations are reported.

S3. Supplementary experimental procedures

S3.1 Derivatization

To measure the enantiomeric excess (*ee*) value of 2-aminohexane product, the reaction mixture was treated according to the previous report.[6] Briefly, the reaction mixture was treated with 12 M HCl (50 μL) and then extracted with EtOAc (2 × 3 mL) to eliminate the unreacted alcohol and ketone. Thereafter, to the aqueous layer, 10 M KOH solution was added to correct the pH over 10 and the free amine was extracted with EtOAc (3 × 3 mL) to obtain the target product. For derivatization, samples in EtOAc were supplemented with acetic anhydride (40 μL) and 4-(N, N-dimethylamino) pyridine (2 mg), then incubated at 25 °C for 1 h and water was added (2 × 500 μL) to hydrolyze the excess amount of acetic anhydride. The organic phase was extracted by EtOAc and dried with anhydrous $MgSO_4$ and filtered before analysis by gas chromatography.

S3.2 Gas chromatography (GC) analysis

Helium was used as carrier gas at a flow rate of 1 mL/min and EtOAc was used as the solvent.

For monitoring the concentrations of (*S*)-2-hexanol, 2-hexanone, and (*R*)-2-aminohexane, GC analysis was executed with the following operation parameters: injector 250 °C; temperature program: 40 °C/hold 8 min; 100 °C/rate 20 °C min^{-1}/hold 1 min; 280 °C/rate 20 °C min^{-1}/hold 1 min.[6]

For determining the *ee* value of 2-aminohexane product, GC analysis was executed with the following parameters: injector 200 °C; temperature program: 60 °C/hold 8 min; 100 °C/rate 5 °C min^{-1}/hold 2 min; 180 °C/rate 10 °C min^{-1}/hold 1 min.[6]

S3.3 Product/cofactor concentration effects on the two fusion enzymes

Product inhibition was determined to measure the initial enzyme activity at different concentrations of (*R*)-2-aminohexane (0 – 30 mM). The initial enzyme activities of SiBP-ADH and SiBP-AmDH were measured according to the

Experimental in the article.

Cofactor concentration effect was determined to measure the initial enzyme activity at different concentrations of NAD(H) (0.5 – 2 mM). The initial enzyme activities of SiBP-ADH and SiBP-AmDH were measured according to the **Experimental** in the article.

S3.4 Stability of SiBP-AmDH

For the assay of thermal stability, biocatalysts containing the same enzyme concentrations (SiBP-AmDH and SiBP-AmDH@SNPs) were incubated in 50 mM Tris-HCl buffer (pH 8.0) at 25 - 80 ^{o}C for 2 h. Residual activities of the enzyme samples were measured at 30 ^{o}C with 2-hexanone as substrate.

For the pH tolerance, biocatalysts containing the same enzyme concentrations (SiBP-AmDH and SiBP-AmDH@SNPs) were incubated in 50 mM buffer solution with different pH values [acetate buffer (pH 4.0 - 5.0), sodium phosphate buffer (pH 6.0 - 7.0), Tris-HCl buffer (pH 8.0 - 9.0), and sodium bicarbonate buffer (pH 10.0 - 11.0)] for 2 h at 25 ^{o}C.

In the above stability assays, the enzyme activity before incubation was defined as 100% for representing the residual activities.

Finally, the long-term storage stability was tested by keeping SiBP-AmDH and SiBP-AmDH@SNPs in 50 mM Tris-HCl buffer (pH 8.0) at 4 ^{o}C for 10 days. The residual activity was compared to the initial enzyme activity defined as 100%.

Residual activities of the above samples were determined according to the **Experimental** in the article.

REFERENCES

1.   H. W. Hoffken, M. Duong, T. Friedrich, M. Breuer, B. Hauer, R. Reinhardt, R. Rabus and J. Heider, *Biochemistry*, 2006, **45**, 82-93.

2.   B. R. Bommarius, M. Schurmann and A. S. Bommarius, *Chem. Commun.*, 2014, **50**, 14953-14955.

3.   J. L. Trompette, M. Clifton and P. Bacchin, *J. Colloid Interface Sci.*, 2005, **290**, 455-461.

4.   M. A. A. Abdelhamid, K. Motomura, T. Ikeda, T. Ishida, R. Hirota and A. Kuroda, *Appl. Microbiol. Biotechnol.*, 2014, **98**, 5677-5684.

5.   W. Bohmer, T. Knaus and F. G. Mutti, *Chemcatchem*, 2018, **10**, 731-735.

6.   G. Q. Zhang, M. B. Quin and C. Schmidt-Dannert, *ACS Catal.*, 2018, **8**, 5611-5620.

7.   J. Liu and Z. Li, *Biotechnol. Bioeng.*, 2019, **116**, 536-542.

8.   S. Mao, J. W. Wang, F. Liu, Z. Zhu, D. Gao, Q. Guo, P. Xu, Z. Ma, Y. Hou, X. Cheng, D. Sun, F. Lu and H. M. Qin, *Microb Cell Fact*, 2018, **17**, 141.

9.   F. G. Mutti, T. Knaus, N. S. Scrutton, M. Breuer and N. J. Turner, *Science*, 2015, **349**, 1525-1529.